

Supramolecular Aggregates of Complex Cations via Unusual Purine–Purine Base Pairing in a New Organorhodium(III) Compound Containing the Antileukemic Drug Purine-6-thione. Synthesis, X-ray Structure of *trans*(C,N⁷),*trans*(S,S),*trans*(P,N⁷)-[Rh(C₆H₅)(H¹,H⁹-H₂tp)₂(PPh₃)] [Rh(C₆H₅)(H¹,H⁹-H₂tp)(H⁹-Htp)(PPh₃)]Cl₃·HCl·6H₂O, and Density Functional Analysis of the {H₂tp···Htp}⁻ Base Pair

Renzo Cini,* Maddalena Corsini,[†] and Alessandro Cavaglioni[‡]

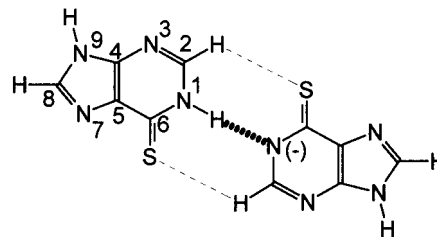
Department of Chemical and Biosystem Sciences and Technologies, University of Siena, Via E. Bastianini 12, I-53100 Siena, Italy

Received July 18, 2000

Introduction

The interest on metal complexes of the often pharmaceutically active derivatives of purine nucleobases increased recently.^{1–6} The reason for these research efforts comes both from the versatility of nucleobase derivatives as ligands^{2,7} and from the search for routes to improve the pharmaceutical properties of certain active drugs.^{1b} For instance, purine-6-thione (H₂tp), an active drug used to cure leukemia in humans, has at least five potential donor atoms (N(1), N(3), N(7), N(9), S(6)). The metal centers, used in the past as Lewis acids to coordinate with purine base derivatives, have been mostly those from the “block d” of the periodic table. In the case the metal is copper or one of the platinum group metals, potential pharmacological activity can come from the oxygen radical scavenger activity⁸ (superoxide dismutase (SOD) like activity) or from the cytostatic activity^{7,9,10} which certain metal-containing functions can exert. Furthermore, purine nucleobases and their derivatives have been, for a long time, recognized as being particularly suited for the formation of a variety of hydrogen bonded pairs.¹¹ The knowledge of the

Scheme 1. Representation of the {H₂tp···Htp}⁻ Base Pairing



base pairing schemes is a key step to understand the conformation and activity of biological molecules. A base pair of the type shown in Scheme 1 and as studied in this work via X-ray diffraction and theoretical tools is quite uncommon.

As a continuation of the research performed in this laboratory since several years, aimed to prepare rhodium and ruthenium complexes containing purine derivatives as ligands, we investigated the reactivity of [RhCl₂(Ph)(PPh₃)₂]¹² with H₂tp. This work led to the isolation and full characterization of the title compound. The X-ray structural study shows the presence of an interesting {H₂tp···Htp}⁻ base pair (Scheme 1) between two complex cations, [Rh(Ph)(H¹,H⁹-H₂tp)₂(PPh₃)]²⁺ and [Rh(Ph)(H¹,H⁹-H₂tp)(H⁹-Htp)(PPh₃)]⁺, which are held together mostly via the N(1)–H···N(1)⁻ hydrogen bond and stacking interactions. We report here on the preparation and on the X-ray diffraction study of this compound as well as on a density functional analysis of the metal free-{H₂tp···Htp}⁻ base pair.

Experimental Section

Materials. RhCl₃·3H₂O (Janssen or Aldrich), SbPh₃ (Fluka), and PPh₃ (Erba) were used as purchased. CH₃OH (MeOH), C₂H₅OH (EtOH), CHCl₃, CH₂Cl₂ and (C₂H₅)₂O (Et₂O) were all analytical grade compounds from C.Erba and were used without any further purification.

Synthesis of [Rh(Ph)(H₂tp)₂(PPh₃)] [Rh(Ph)(H₂tp)(Htp)(PPh₃)]Cl₃·HCl·6H₂O (2). An amount of 78 mg (0.1 mmol) [RhCl₂(Ph)(PPh₃)₂] (1), (prepared as previously reported in ref 12) was suspended in 6 mL of MeOH together with 30 mg (0.2 mmol) of H₂tp. The resulting suspension was refluxed for 3 h. The color turned from red to yellow, and a clear solution was obtained. The solvent was in part removed in a vacuum to a final solution volume of ca. 2 mL; then Et₂O (30 mL) was added at once: a yellow precipitate formed, which was filtered off, washed three times with CH₂Cl₂, and then dried in an air atmosphere at 25 °C for 12 h. The crude compound was re-crystallized twice from MeOH/Et₂O mixtures. Single, yellow crystals were obtained by slowly evaporating a solution of the crude product in EtOH/MeOH 1:1, v/v. Yield: 52 mg, 60%. Anal. Calcd. for C₆₈H₆₈Cl₄O₆N₁₆P₂Rh₂S₄ (mw, 1742.6): C, 46.87; H, 3.93; N, 12.86, S, 7.36, Cl, 8.14. Found: C, 47.60; H, 3.86; N, 12.94, S, 7.35, Cl, 8.24. ¹H NMR ((CD₃)₂SO): 8.712 ppm (s, 1H, H(8) pu(2)), 8.558, 8.539 (s, s, 2H, H(2) pu(2), H(8) pu(1)), 7.50–7.10 (m, 15H, PPh₃), 7.016 (d, 2H, η¹-Ph(ortho)), 6.60–6.75 (m, 3H, η¹-Ph(para, meta)). ¹H NMR (CD₃OD): 8.822 ppm (s, 1H, H(8) pu(2)), 8.582 (s, 2H, H(2) pu(2), H(8) pu(1)), 8.554 (s, 1H, H(2) pu(1)), 7.50–7.20 (m, 15H, PPh₃), 7.092 (d, 2H, η¹-Ph(ortho)), 6.70–6.90 (m, 3H, η¹-Ph(para, meta)). IR: 1626 cm⁻¹ (s), 1582 (m), 1234 (s), 1091 (m), 1018 (m), 854 (s), 734 (s), 699 (s), 535 (s).

X-ray Structure Determination. A well-formed yellow crystal of 2 (prism, 0.15 × 0.20 × 0.30 mm) was used for the diffraction study, through a Siemens P4 diffractometer. Accurate cell constants (Table 1) were determined by using the full-matrix least-squares refinement

[†] Author contributed to density functional analysis.

[‡] Author contributed to synthesis and crystal growth.

- (1) (a) Zhu, F.-C.; Schmalke, H. W.; Fischer, B.; Dubler, E. *Inorg. Chem.* **1998**, *37*, 1161. (b) Dubler, E. *Metal Ions in Biological Systems*; Sigel, A., Sigel, H., Eds.; M. Dekker Inc.: Basel, 1996; Vol. 32, Chapter 8.
- (2) Yamanari, K.; Fukuda, I.; Kawamoto, T.; Kushi, Y.; Fuyuhiko, A.; Kubota, N.; Fukuo, T.; Arakawa, R. *Inorg. Chem.* **1998**, *37*, 5611.
- (3) Garcia-Raso, A.; Fiol, J. J.; Bádenas, F.; Cons, R.; Terrón, A.; Quirós, M. *J. Chem. Soc., Dalton Trans.* **1999**, 167.
- (4) (a) Cini, R.; Grabner, S.; Bukovec, N.; Cerasino, L.; Natile, G. *Eur. J. Inorg. Chem.* **2000**, 1601. (b) Bellucci, C.; Cini, R. *J. Inorg. Biochem.* **1999**, *76*, 243. (c) Cini, R.; Pifferi, C. *J. Chem. Soc., Dalton Trans.* **1999**, 699. (d) Cavaglioni, A.; Cini, R. *J. Chem. Soc., Dalton Trans.* **1997**, 1149. (e) Cini, R.; Bozzi, R.; Karaulov, A.; Hursthouse, M. B.; Calafat, A. M.; Marzilli, L. *G. Chem. Commun.* **1993**, 899.
- (5) Cavallo, L.; Cini, R.; Kobe, J.; Marzilli, L. G.; Natile, G. *J. Chem. Soc., Dalton Trans.* **1991**, 1867.
- (6) (a) Grabner, S.; Plavec, J.; Bukovec, N.; Di Leo, D.; Cini, R.; Natile, G. *J. Chem. Soc., Dalton Trans.* **1998**, 1447. (b) Sinur, A.; Grabner, S. *Acta Crystallogr.* **1995**, C51, 1769.
- (7) Lippert, B., Ed. *Cisplatin. Chemistry and Biochemistry of a Leading Anticancer Drug*; Wiley-VCH: Weinheim, 1999.
- (8) Cini, R. *Commun. Inorg. Chem.* **2000**, *000*, 000.
- (9) Bierbach, U.; Sabat, M.; Farrell, N. *Inorg. Chem.* **2000**, *39*, 1882.
- (10) Marzilli, L. G.; Ano, S. O.; Intini, F. P.; Natile, G. *J. Am. Chem. Soc.* **1999**, *121*, 9133.

(11) Saenger, W. *Principles of Nucleic Acid Structure*; Springer-Verlag: Heidelberg, 1983.

(12) Cini, R.; Cavaglioni, A. *Inorg. Chem.* **1999**, *38*, 3751.

Table 1. Selected Crystal Data and Structure Refinement for $[\text{Rh}(\text{Ph})(\text{H}_2\text{tp})_2(\text{PPh}_3)][\text{Rh}(\text{Ph})(\text{H}_2\text{tp})(\text{Htp})(\text{PPh}_3)]\text{Cl}_3 \cdot \text{HCl} \cdot 6\text{H}_2\text{O}$ (2)

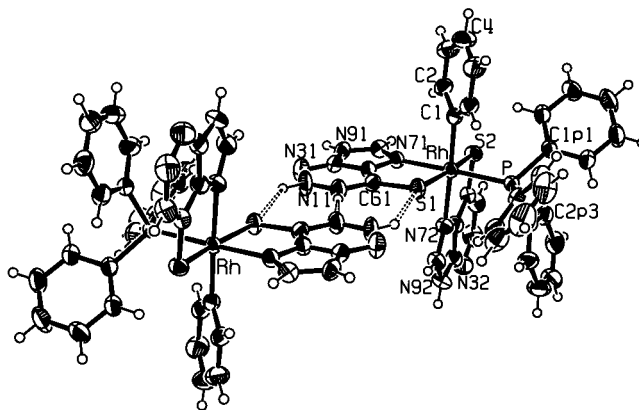
parameter	value
emp form	$\text{C}_{68}\text{H}_{68}\text{Cl}_4\text{N}_{16}\text{O}_6\text{P}_2\text{Rh}_2\text{S}_4$
form wt	1743.18
wavelength/Å	0.71073
cryst syst, space group	triclinic, $P(-1)$ (No. 2)
$a/\text{Å}$	10.507(2)
α/deg	81.21(1)
$b/\text{Å}$	12.596(1)
β/deg	80.64(1)
$c/\text{Å}$	15.339(2)
γ/deg	81.52(1)
vol/Å ³	1963.8(5)
Z , $d_{\text{calc}}/\text{Mg m}^{-3}$	1, 1.474
reflns collect/unique	7312/6907 [R(int) = 0.0263]
refinement method	full-matrix least-squares on F^2
data/restraints/params	6907/0/470
Final R indices [$I > 2\sigma(I)$]	$R1 = 0.0496$, $wR2 = 0.1097$
R indices (all data)	$R1 = 0.0841$, $wR2 = 0.1239$

of the values of 24 carefully centered randomly selected reflections ($10 < 2\theta < 32^\circ$). The diffraction data set (20°C) was corrected for Lorentz-polarization and absorption effects. The solution and refinement of the structure (based on F^2 ; space group $P(-1)$, No. 2) were performed through Patterson and Fourier synthesis methods, and full-matrix least-squares cycles. The asymmetric unit contains a complex molecule, 1.5 Cl^- ions, 0.5 HCl molecule, and 3 H_2O molecules. All of the H-atoms of the complex molecule were set in calculated positions and allowed to ride on the atoms to which they are bound during the subsequent cycles of refinement. The intermolecular $\text{N}(11) \cdots \text{N}(11)$ ($-x, -y + 2, -z$) contact distance at this stage of refinement was 2.71(1) Å; the two purine (pu) systems being coplanar. This means that both the N(11) atoms of the adjacent molecules cannot be protonated and that an $\text{N}-\text{H} \cdots \text{N}$ hydrogen bond exists. As a consequence, the H(11) atom was given 0.5 occupancy. Once all non-hydrogen atoms from the complex molecule and one Cl^- anion were located, three new peaks were assigned as oxygen atoms from cocrystallized water molecules on the basis of the exam of the interatomic contact distances and the peak heights. At this stage, the Fourier difference map showed two new broad peaks, which were interpreted as two chlorine atoms (Cl(2A) and Cl(2B)) at 0.5 occupancy each. The refined thermal ellipsoids for Cl(2A) and Cl(2B) are elongated. The exam of the contact distances suggests that the residual proton may reside on the latter chlorine atoms (it has been assumed that its occupancy is 0.25 on each Cl). The subsequent refinement cycles brought to convergence and to reasonable contact distances for the water molecules, the Cl^- anions and the HCl molecules. The H-atoms of the water molecules and that of the HCl molecules were not included at all. All the non-hydrogen atoms were treated as anisotropic whereas the H-atoms were considered isotropic.

All calculations were performed by using SHELX 97¹³ and PARST 97;¹⁴ the graphics outputs were obtained through the XPM-A-ZORTEP¹⁵ and ORTEP32¹⁶ packages implemented on PC-Pentium machines.

Spectroscopy. ¹H NMR spectra of **2** were recorded from freshly prepared $(\text{CD}_3)_2\text{SO}$ or CD_3OD (0.01 mol dm^{-3}) solutions through a Bruker AC-200 spectrometer working at 200 MHz and 25°C . IR spectra from Nujol mull in the range of $4000\text{--}400 \text{ cm}^{-1}$ were recorded on a Perkin-Elmer 1800 spectrometer.

Density Functional Analysis. All density functional calculations have been performed by using the GAUSSIAN94/DFT¹⁷ package implemented on an SGI Origin 2000 machine. Geometry optimizations, energy calculations, and population analysis have been obtained by

**Figure 1.** Drawing of the $\{[\text{Rh}(\text{Ph})(\text{H}^1, \text{H}^9\text{-H}_2\text{tp})_2(\text{PPh}_3)]^+ \cdots [\text{Rh}(\text{Ph})(\text{H}^1, \text{H}^9\text{-H}_2\text{tp})(\text{H}^9\text{-Htp})(\text{PPh}_3)]^{3+}\}$ aggregate. The ellipsoids enclose 30% probability.

using the B3LYP¹⁸ method and the 6-31G**¹⁷ basis set. All geometrical parameters were fully optimized without symmetry constraints. Other details are as those reported in ref 19. The molecules optimized were $\text{H}^1, \text{H}^9\text{-H}_2\text{tp}$, $\text{H}^1, \text{H}^7\text{-H}_2\text{tp}$, $\text{H}^9\text{-Htp}^-$, $\text{H}^1\text{-Htp}^-$, $\{\text{H}^1, \text{H}^9\text{-H}_2\text{tp} \cdots \text{H}^9\text{-Htp}\}^-$, $\text{H}_2\text{C}=\text{S}$, $\text{CH}_2=\text{NH}$, and $\{\text{H}_2\text{C}=\text{S} \cdots \text{HC}(\text{H})=\text{NH}\}$. No correction for the basis set superposition error was applied for the computations of the reaction energies of the formal reactions from the overall electronic energies, at this preliminary stage.

Results and Discussion

Reactivity of $[\text{RhCl}_2(\text{Ph})(\text{PPh}_3)_2]$ with Purine-6-thione. The reaction of *trans*- $[\text{RhCl}_2(\text{Ph})(\text{PPh}_3)_2]$ (**1**) with H_2tp (1:2 molar ratio) in MeOH produced the $[\text{Rh}(\text{Ph})(\text{H}_2\text{tp})_2(\text{PPh}_3)]^{2+}$ and $[\text{Rh}(\text{Ph})(\text{H}_2\text{tp})(\text{Htp})(\text{PPh}_3)]^+$ molecules through removal of the chloride anions from the coordination sphere of Rh(III). It is reasonable to assume that the presence of a vacant site *trans* to Ph in the coordination sphere of **1** (ref 12) facilitates the attack of the first H_2tp molecule to rhodium via the N(7) atom (see Supporting Material, Scheme 1S). The subsequent step is the removal of one chloride anion and the formation of a Rh–S bond. The replacement of the residual chloride anion and of one PPh_3 ligand is facilitated by the high *trans*-effect/influence from S and P atoms and by the steric repulsion from PPh_3 .

X-ray Structure of $[\text{Rh}(\text{Ph})(\text{H}_2\text{tp})_2(\text{PPh}_3)][\text{Rh}(\text{Ph})(\text{H}_2\text{tp})(\text{Htp})(\text{PPh}_3)]\text{Cl}_3 \cdot \text{HCl} \cdot 6\text{H}_2\text{O}$. The structure of the aggregate of the complex cations of **2** is represented in Figure 1; selected geometrical parameters for the asymmetric unit are listed in Tables 2 and 3. The coordination sphere around the metal is pseudo-octahedral, and the two purine-6-thione ligand molecules act as chelators through the N(7) and S atoms. The two S atoms are *trans* to each other. Two *cis* sites are occupied by the N(7) atoms which are *trans* to a P(Ph_3) atom and to a C(Ph) atom, respectively.

The Rh–P bond distance is 2.3025(14) Å, significantly shorter than the value previously found for **1** (2.3635(9) Å¹²) and in agreement with a smaller *trans*-influence by nitrogen when compared to phosphorus. The two Rh–S bond distances

(13) Sheldrick, G. M. *SHELX 97, Program for the Refinement of Crystal Structures*; University of Göttingen: Germany, 1997.

(14) Nardelli, M. *PARST 97, A System of Computer Routines for Calculating Molecular Parameters from Results of Crystal Structure Analyses*; University of Parma: Italy, 1997.

(15) Zsolnai, L. *XPM-A-ZORTEP 98*; University of Heidelberg: Germany, 1998.

(16) Johnson, C. K.; Burnett, M. N. *ORTEP-3 for Windows*; Oak Ridge National Laboratory: Oak Ridge, TN, 1998. 32-bit Implementation by Farrugia, L. J., University of Glasgow.

(17) Frisch, M. J.; Trucks, G. W.; Schlegel, H. B.; Gill, P. M. W.; Johnson, B. G.; Robb, M. A.; Cheeseman, J. R.; Keith, T.; Petersson, G. A.; Montgomery, J. A.; Raghavachari, K.; Al-Laham, M. A.; Zakrzewski, V. G.; Ortiz, J. V.; Foresman, J. B.; Cioslowski, J.; Stefanov, B. B.; Nanayakkara, A.; Challacombe, M.; Peng, C. Y.; Ayala, P. Y.; Chen, W.; Wong, M. W.; Andres, J. L.; Replogle, E. S.; Gomperts, R.; Martin, R. L.; Fox, D. J.; Binkley, J. S.; Defrees, D. J.; Baker, J.; Stewart, J. P.; Head-Gordon, M.; Gonzalez, C.; Pople, J. A. *Gaussian, Inc.*: Pittsburgh, PA, 1995.

(18) (a) Becke, A. D. *J. Chem. Phys.* **1988**, *88*, 1053. (b) Lee, C.; Yang, W.; Parr, R. G. *Phys. Rev.* **1988**, *B37*, 785.

(19) Cini, R. *J. Biomol. Struct. Dyn.* **1999**, *16*, 1225.

Table 2. Selected Bond Lengths (Å) and Angles (deg) for [Rh(Ph)(H₂tp)₂(PPh₃)] [Rh(Ph)(H₂tp)(Htp)(PPh₃)]Cl₃·HCl·6H₂O 2^a

vectors	length/angle
Rh–C(1)	2.030(5)
Rh–N(71)	2.122(4)
Rh–N(72)	2.191(4)
Rh–P	2.3025(14)
Rh–S(1)	2.3851(14)
Rh–S(2)	2.4118(14)
S(1)–C(61)	1.709(5)
S(2)–C(62)	1.711(5)
S(2)–Rh–S(1)	171.91(5)
P–Rh–S(1)	97.32(5)
P–Rh–S(2)	90.33(5)
N(71)–Rh–S(1)	84.81(12)
N(72)–Rh–S(1)	91.44(12)
N(71)–Rh–S(2)	87.44(12)
N(72)–Rh–S(2)	85.79(12)
C(1)–Rh–S(1)	89.89(14)
C(1)–Rh–S(2)	92.50(15)
N(71)–Rh–P	176.79(12)
N(72)–Rh–P	90.91(11)
C(1)–Rh–P	91.85(14)
N(71)–Rh–N(72)	86.62(16)
C(1)–Rh–N(71)	90.56(18)
C(1)–Rh–N(72)	176.76(19)

are 2.4118(14) and 2.3851(14) Å. The values are close to the Rh–S (trans to Sb) bond length (2.403(2) Å) for [RhCl(Ph)(H₂tp)(SbPh₃)].^{4d} The Rh–N(71) (trans to P) bond distance is 2.122(4) Å, longer than the expected value for a Rh(III)–N(sp²) (trans to N) linkage.^{20,21} The Rh–N(72) (trans to C) bond length is 2.191(4) Å, longer than the Rh–N(71) bond because of the high trans-influence by Ph. The bond angles around the metal atom are close to the idealized values of 90 and 180° with the exception of the S(1)–Rh–S(2) angle (171.91(5)°) and the chelation angles S–Rh–N (85.79(12), 87.44(12)°). The rhodium atom deviates 0.1080(5) Å from the plane defined by C(1), S(1), S(2) and N(72) (toward P).

The Purine Ligand. The S(6)/N(7) bite distances reflect the different Rh–N bond strength found for the two purine moieties; they are 3.065(5) and 3.118(5) Å. It has to be noted that the S(6)/N(7) bite is common in contrast to an O(6)/N(7) bite,²² for purine derivatives. The purine(2) (pu(2)) ligand is fully protonated at N(1) and N(9); whereas pu(1) is fully protonated at N(9) and to 50% at N(1). This allows a pu···pu base pairing via a N(11)–H···N(11)[–] hydrogen bond (N···N (–x, –y + 1, –z), 2.708(7) Å, see Figure 1). As a consequence the structure consists of supramolecular aggregates of complex cations. The observation of the unusual hydrogen bond between the purine-6-thione ligands suggested to perform a density functional analysis on metal-free purine-6-thione systems (see below), with the aim to compute the structure and energetics of the base pair. The C(2)–N(1)–C(6) bond angle, which is sensible to the protonation status of N(1),²³ has values of 120.3(5)° (pu(1)) and 120.4(5)° (pu(2)). The C–S bond lengths average 1.718(5) Å and show that the thione structure of the ligand is maintained in the chelate. The H₂tp(2) ligand has an extensive intramolecular stacking interaction (Figure 2a) with the C(1P3)/C(6P3) phenyl ring of PPh₃; angle between the two least-squares planes, 14.6(2)°; shortest interatomic contact, 3.106(7) Å (N(72)···C(1P3)).

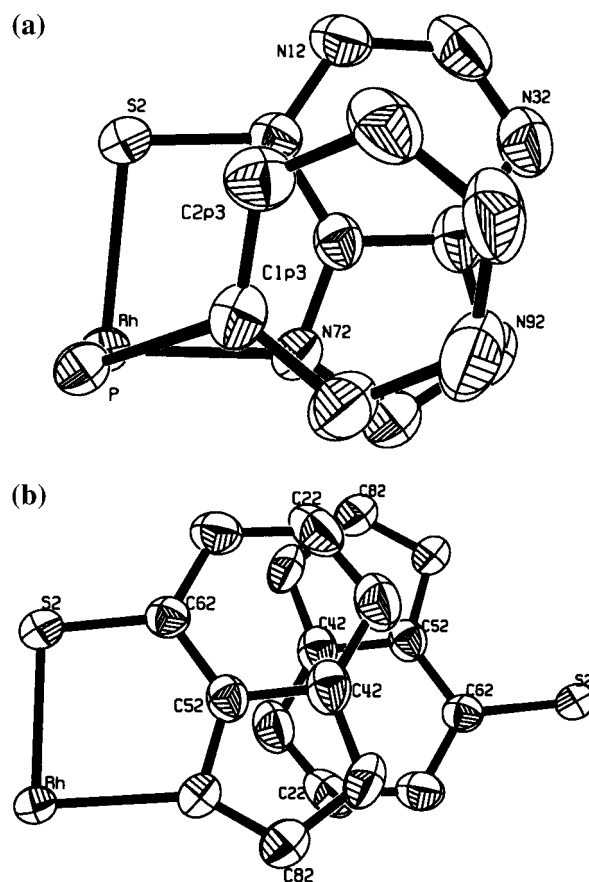


Figure 2. (a) The drawing shows the intramolecular stacking interaction between the H₂tp(2) ligand and the C(1P3)/C(6P3) phenyl ring of PPh₃. (b) The drawing shows the intermolecular stacking interaction between the H₂tp(2) (x, y, z) and H₂tp(2) (–x + 1, –y + 1, –z) π -systems. The fragment is viewed along an axis perpendicular to the plane defined by the atoms of H₂tp(2).

Crystal Packing. Some intermolecular stacking interactions occur between pu(1) (x, y, z) and pu(1) (–x + 1, –y + 2, –z); the atoms involved are C(81), N(91), C(41), and C(31) for both the purine systems but the overlapping region is small. More extensive intermolecular stacking interactions occur between two pu(2) moieties (at x, y, z and –x + 1, –y + 1, –z) (see Figure 2b) which involve both the pyrimidine and imidazole moieties: the shortest interatomic contact is C(52)···N(32), 3.351(7) Å.

The purine nitrogen atoms, the chloride anions, and HCl and H₂O molecules are part of the network of hydrogen bonds. Selected interactions are as follows (the N(11)–H···N(11) interaction has been presented above). N(91) is linked to O(3W) (–x + 1, –y + 1, –z) (N···O, 2.767(7) Å; N–H···O, 159(1)°). N(12) interacts with O(1W) (–x + 1, –y + 1, –z + 1) (N···O, 2.770(7) Å; N–H···O, 152(1)°). N(92) links Cl(1) (x, y, z + 1) (N···Cl, 3.140(5) Å; N–H···Cl, 174.7(8)°). Cl(1) interacts also with O(1W), O(2W), and O(3W), the Cl···O distances ranging from 3.062(8) to 3.763(10) Å. Cl(2A) and Cl(2B) (which are assumed as partially protonated) have short contacts to O(2W) and O(3W) in the range of 2.91(2)–3.69(3) Å. Finally, it is interesting to note that the aggregates are connected with each other via stacking interactions in a way to form infinite chains which in turn are connected to each other via a network of hydrogen bonds with Cl[–], H₂O, and HCl.

Density Functional Analysis. Examination of the geometrical parameters for the optimized structures for a series of purine-6-thione systems (see Table 3 for a list of selected values) shows a very good agreement with the corresponding values previously

(20) Frei, C.; Zilian, A.; Raselli, A.; Güdel, H. U.; Bürgi, H.-B. *Inorg. Chem.* **1992**, *31*, 4762.

(21) Maeder, U.; von Zelewsky, A.; Stoeckli-Evans, H. *Helv. Chim. Acta* **1992**, *75*, 1320.

(22) Sigel, H.; Massoud, S. S.; Corfù, N. A. *J. Am. Chem. Soc.* **1994**, *116*, 2958.

(23) Singh, C. *Acta Crystallogr.* **1965**, *19*, 861.

Table 3. Selected Bond Distances (Å) and Bond Angles (deg) for Purine-6-thione in Different Forms and for the Base-Paired System $\{H^1, H^9-H_2tp \cdots H^9-Htp\}^-$ ^a

vectors	H ¹ ,H ⁹ -H ₂ tp	H ¹ ,H ⁷ -H ₂ tp ^b	H ¹ -Htp ⁻	H ⁹ -Htp ⁻	$\{H^1, H^9-H_2tp \cdots H^9-Htp\}^-$ ^c	
N(1)–C(2)	1.363	1.374 (1.350)	1.372	1.329	1.357 (1.365(7))	1.342 (1.356(7))
C(2)–N(3)	1.305	1.300 (1.307)	1.300	1.349	1.320 (1.314(8))	1.338 (1.316(8))
N(3)–C(4)	1.358	1.367 (1.364)	1.375	1.341	1.350 (1.343(7))	1.342 (1.356(7))
C(4)–C(5)	1.401	1.403 (1.397)	1.441	1.404	1.400 (1.378(7))	1.402 (1.369(7))
C(5)–C(6)	1.432	1.414 (1.396)	1.412	1.437	1.432 (1.385(7))	1.431 (1.380(7))
C(6)–S	1.661	1.672 (1.676)	1.702	1.706	1.678 (1.711(5))	1.707 (1.709(5))
C(6)–N(1)	1.408	1.394 (1.384)	1.399	1.381	1.394 (1.344(6))	1.380 (1.359(6))
C(5)–N(7)	1.377	1.370 (1.370)	1.368	1.392	1.385 (1.370(6))	1.390 (1.366(6))
N(7)–C(8)	1.310	1.368 (1.346)	1.340	1.307	1.308 (1.317(6))	1.308 (1.310(6))
C(8)–N(9)	1.381	1.320 (1.326)	1.363	1.383	1.382 (1.356(7))	1.383 (1.368(6))
N(9)–C(4)	1.369	1.371 (1.363)	1.347	1.383	1.375 (1.363(7))	1.380 (1.353(7))
C(6)–N(1)–C(2)	126.5	125.3 (125.4)	125.8	120.5	125.5 (120.4(5))	121.4 (120.3(5))
N(1)–C(2)–N(3)	124.7	125.3 (125.0)	124.9	130.3	125.4 (128.1(6))	128.7 (128.1(5))
C(2)–N(3)–C(4)	111.8	113.7 (113.0)	113.6	109.2	111.3 (110.9(5))	110.2 (111.8(5))
N(3)–C(4)–C(5)	128.3	123.2 (124.2)	124.6	127.9	128.3 (125.5(6))	123.8 (123.4(5))
N(3)–C(4)–N(9)	126.5	126.2 (125.9)	125.9	126.8	126.4 (129.8(5))	126.9 (130.9(5))
C(4)–C(5)–C(6)	119.1	123.5 (121.9)	120.3	117.8	118.7 (120.3(5))	117.8 (122.6(5))
C(5)–C(6)–N(1)	109.6	109.1 (110.4)	110.8	114.4	110.8 (114.6(5))	114.1 (113.7(5))
S–C(6)–C(5)	130.0	127.8 (127.0)	131.5	124.4	126.7 (120.1(4))	124.0 (119.8(4))
C(6)–C(5)–N(7)	130.3	131.2 (132.2)	131.2	132.1	130.8 (128.3(5))	131.9 (126.4(5))
C(5)–N(7)–C(8)	104.7	106.2 (106.1)	101.7	105.0	104.7 (104.1(4))	104.8 (104.5(4))
N(7)–C(8)–N(9)	113.1	113.5 (113.6)	118.8	113.3	113.2 (112.4(5))	113.3 (112.2(5))
C(8)–N(9)–C(4)	106.4	104.3 (104.5)	101.5	106.3	106.4 (107.4(5))	106.3 (106.7(4))

^a The molecules were geometry optimized at the DFT-B3LYP/6-31G ** level. Values in parentheses are from X-ray analyses at the solid state.

^b See ref 24 for the experimental values. The reported estimated standard deviations are 0.002 Å and 0.1°. ^c The experimental values are those for **2** from this work.

found in the solid state through X-ray diffraction for H¹,H⁷-H₂tp²⁴ and for the paired purine-6-thione systems found in this work for **2**; the computed C–N or C–C bond distances for H¹,H⁷-H₂tp are in some cases slightly larger than the experimental ones (largest difference, 0.024 Å). This effect was previously noted for other molecules computed at similar levels of theory (see for instance ref 25). The computed values for the S–C(6)–C(5) angles for metal free $\{H^1, H^9-H_2tp \cdots H^9-Htp\}^-$ are larger by some 5.8° than the corresponding values found for **2** because of the S,N⁷-chelation. The computed N(1)⋯N(1) contact distance for metal free $\{H^1, H^9-H_2tp \cdots H^9-Htp\}^-$ (2.813 Å) is larger by some 0.1 Å than the corresponding value found for metal bound $\{H^1, H^9-H_2tp \cdots H^9-Htp\}^-$. It has to be noted that DFT methods at the BLYP and B3LYP levels have been considered to reproduce hydrogen bonds accurately.²⁶ The

discrepancy found for the N(1)⋯N(1) distance is probably ascribable to metal ligation and packing forces. The computed C(6)–S and C(2)–H bond distances for both H¹,H⁹-H₂tp and H⁹-Htp⁻ increase slightly upon aggregate formation. This effect suggests that two C(2)–H⋯S hydrogen bond-like interactions can occur. The H⋯S contact distances from theory are in fact 2.563 (S from H⁹-Htp⁻) and 2.923 Å, i.e., smaller than the sum of the van der Waals radii (3.0–3.25 Å).²⁷

The computed deprotonation energy for the formal reaction from H¹,H⁹-H₂tp to H¹-Htp⁻ (342.664 kcal) is smaller than that to H⁹-Htp⁻ (349.705 kcal); notwithstanding, deprotonation occurs at N(1) instead of N(9) for pu(1) of **2**, due to the electronic effects of the metal ligation. The computed energy for the formal conversion of H¹,H⁹-H₂tp to H¹,H⁷-H₂tp is –3.119 kcal, i.e., the shift of a proton from H⁷ to H⁹ is a small energy

(24) Sletten, E.; Sletten, J.; Jensen, L. H. *Acta Crystallogr.* **1969**, B25, 1330.

(25) Cini, R.; Musaev, D. G.; Marzilli, L. G.; Morokuma, K. *J. Mol. Struct. (Theochem.)* **1997**, 392, 55.

(26) Koch, W.; Holthausen, M. C. *A Chemist's Guide to Density Functional Theory*; Wiley-VCH: Weinheim, 2000.

(27) Bondi, A. *J. Phys. Chem.* **1964**, 68, 441.

barrier for the S,N⁷-chelation process. It is also worth to note that purine-6-thione has been found only as H¹,H⁷-H₂tp at the solid state.²⁴ The {H¹,H⁹-H₂tp...H⁹-Htp}⁻ aggregate has a formation energy from the isolated moieties of -27.912 kcal, which compares well with computed values for guanine-cytosine Watson-Crick pairing energies at the MP2/6-31G* level.²⁸ The computed total pairing energy comes mostly from the N-H...N⁻ interaction. To evaluate the contribution of the two C-H...S interactions, the model systems H₂C=S, H₂C=NH, and {H₂C=S...HC(H)=NH} were analyzed. In fact, the computed formation energy (uncorrected) for the {CH₂S...HC(H)=NH} aggregate is as small as -0.389 kcal.

In conclusion the work showed at least the following points. First, the reactivity of [RhCl₂(Ph)(PPh₃)₂] with H₂tp (in alcohol) is quite different from that of the homologous [RhCl₂(Ph)-(SbPh₃)₃].^{4d} It is possible that the chloride ligands of [RhCl₂(Ph)(PPh₃)₂] are activated by (PPh₃)C-H...Cl hydrogen bonds.¹² Such types of interactions have been postulated to play important roles on the reactivity of coordination and organometallic compounds.²⁹ Second, the metal coordination to purine derivatives can tune deprotonation of the ligand through electron withdrawing effects as shown also from other cases;³⁰ indeed, pu(1) of **2**, which undergoes the deprotonation at N(1), is more

tightly bound to the metal than pu(2). Third, the metal facilitated deprotonation of purine bases can trigger unusual types of base pairing, such as {H¹,H⁹-H₂tp...H⁹-Htp}⁻; this, in turn, can direct the formation of supramolecular aggregates. Fourth, the pairing of purine-6-thione bases of the type {H¹,H⁹-H₂tp...H⁹-Htp}⁻ is estimated to be at least as strong as the GC-Watson-Crick base pairing; the bonding strength mostly comes from the N(1)-H...N(1)⁻ hydrogen bond.

Acknowledgment. Mr. F. Berrettini is acknowledged for the X-ray data collection at Centro Interdipartimentale di Analisi e Determinazioni Strutturali (CIADS), Università di Siena. Consorzio Interuniversitario per il Calcolo Automatico (CINECA, Bologna) is acknowledged for a grant which allowed the DFT calculations. Ministero dell'Università e della Ricerca Scientifica e Tecnologica (MURST, Roma), Consiglio Nazionale delle Ricerche (CNR, Roma) and Università di Siena, are acknowledged for funding.

Supporting Information Available: An X-ray crystallographic file in CIF format for the structure of **2**. Atomic coordinates and displacement parameters, full tables of bond lengths and angles. Scheme of the proposed mechanism for the reaction of **1** and purine-6-thione. This material is available free of charge via the Internet at <http://pubs.acs.org>.

IC000814G

(28) Scheiner, S. *Hydrogen Bonding A Theoretical Perspective*; Oxford University Press: Oxford, 1997.

(29) Huang, L.-Y.; Aulwurm, U. R.; Heinemann, F. W.; Knoch, F.; Kisch, H. *Chem. Eur. J.* **1998**, *4*, 1641.

(30) Song, B.; Zhao, J.; Griesser, R.; Meiser, C.; Sigel, H.; Lippert, B. *Chem. Eur. J.* **1999**, *5*, 2374.